Available online at www.sciencedirect.com
SCIENCE DIRECT®
European Polymer Journal 42 (2006) 655–662
EUROPEAN POLYMER JOURNAL
www.elsevier.com/locate/europolj

Morphology, isothermal and non-isothermal crystallization kinetics of poly(methylene terephthalate)

Mingtao Run *, Chenguang Yao, Yingjin Wang

College of Chemistry and Environmental Science, Hebei University, Hezuo Road No. 88, Baoding 071002, China

Received 26 April 2005; received in revised form 8 August 2005; accepted 12 August 2005
Available online 26 September 2005

Abstract

The morphology of crystals, isothermal and non-isothermal crystallization of poly(methylene terephthalate) (PMT) have been investigated by using polarized optical microscopy and differential scanning calorimeter (DSC). The POM photographs displayed only several Maltese cross at the beginning short time of crystallization indicating that some spherulites had been formed. The crystal cell belonged to the Triclinic crystal systems and the cell dimensions were calculated from the WAXD pattern. The commonly used Avrami equation and that modified by Jeziorny were used, respectively, to fit the primary stage of isothermal and non-isothermal crystallization. The Ozawa theory was also used to analyze the primary stage of non-isothermal crystallization. The Avrami exponents n were evaluated to be in the range of 2–3 for isothermal crystallization, and 3–4 for non-isothermal crystallization. The Ozawa exponents m were evaluated to be in the range of 1–3 for non-isothermal crystallization in the range of 135–155 °C. The crystallization activation energy was calculated to be −78.8 kJ/mol and −94.5 kJ/mol, respectively, for the isothermal and non-isothermal crystallization processes by the Arrhenius' formula and the Kissinger's methods.

Keywords: Poly(methylene terephthalate); Crystallization; Differential scanning calorimeter; Polarized optical microscopy; Avrami

1. Introduction

Poly(methylene terephthalate) (PMT) is one of aromatic polyesters with the following chemical structure: 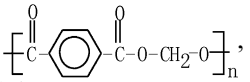 , which had been synthesized in 1982 [1,2]. However, as a kind of polyesters, PMT cannot be prepared by conventional processes as the conventional polyesters, such as PET and PBT [3–6]. PMT is synthesized as white powders via the reaction of cesium or potassium terephthalates with dibromomethane or bromochloromethane in *N*-methylpyrrolidone at temperatures of 80–125 °C. Compared to the molecular chain of PBT with four methylene $(-CH_2-)_4$ in its repeated unit, PMT has only one $-CH_2-$ in its repeated unit of molecular chains segments. Although PMT possesses poor thermal stability and decomposes rapidly during the melting process, it can yield quantitative short filaments spun from the melt of products. PMT may be viewed as a candidate of higher strength and modulus material due to its high density of phenyl in its molecular chains.

* Corresponding author. Fax: +86 312 5079525.
E-mail address: rmthyp@hotmail.com (M. Run).

0014-3057/$ - see front matter © 2005 Elsevier Ltd. All rights reserved.
doi:10.1016/j.eurpolymj.2005.08.010

In general, the final properties of a crystalline polymer have close relationship with its crystallinity, crystalline morphology and crystalline structure, and these have been decided by processing conditions. A great deal of efforts has been made on studying the crystallization kinetics of polyesters corresponding to their change of the performed properties [7,8]. Hence, it is very important to study the crystallization behavior of the PMT. East et al. [2] have found that the polymer sample were largely crystalline and the amorphous sample could show clear T_g, $T_{c,c}$ and T_m transitions. To our best knowledge, few reports on the crystal morphology and crystallization behaviors of PMT have been found in literature.

The crystal morphology, isothermal and non-isothermal crystallization kinetics of the PMT are investigated in this article. From DSC measurements, the study on the isothermal and non-isothermal crystallization kinetics is performed through the Avrami theory and other equations, and the crystallization activation energy is also calculated by different methods.

2. Experimental

2.1. Materials

The white powder of PMT was received from the College of Textile Industries of North Carolina University and its melting point T_m and melt-crystallization temperature T_c were 245.1 and 192.8 °C, respectively. The sample was dried in a vacuum oven at 140 °C for 12 h before being used in POM, WAXD and DSC measurements.

2.2. Polarized optical microscopy (POM)

The morphology of PMT crystals was studied with a Leitz SM-LUX-POL polarized optical microscopy equipped with a hot-stage and a camera system. The sample was prepared by sandwiching a tiny pellet of PMT powder between two glass plates with a distance of 100 μm, compressing at 260 °C for 1 min and then annealing at 200 °C on hot-stage and then took photographs at different time by the camera.

2.3. Wide-angle X-ray diffraction (WAXD)

The WAXD pattern of PMT was recorded on a Rigaku D/MAX-2500UBZ+/PCD diffractometer system. Nickel-filtered CuKα ($\lambda = 0.15406$ nm) radiation generated at 40 kV and 200 mA was used. The diffraction pattern was recorded from 2θ scans in the range of 3–80° at a scanning speed of 10°/min.

2.4. Differential scanning calorimetry (DSC)

The isothermal crystallization processes were performed by the Perkin–Elmer DSC-7 instrument as following: the sample was heated to 260 °C at 80 °C/min under a nitrogen atmosphere, held for 2 min and then cooled at 200 °C/min to the designated crystallization temperatures (T_c) rapidly.

The non-isothermal crystallization behaviors of PMT were performed as following: the sample was heated to 260 °C in nitrogen, held for 2 min and then cooled to 50 °C at constant cooling rates of 10, 15, 20, 30 °C/min. The exothermic curves of heat flow as a function of time were recorded and investigated.

3. Results and discussion

3.1. The spherulitic morphology

After annealing at 200 °C for 2 min, the crystal morphology of PMT is observed by POM and an image is obtained as shown in Fig. 1(A). Within the volume between two glass plates with a distance about 100 μm, several small Maltese crosses with the size of 2–4 μm can be observed in Fig. 1(A) as the arrow pointed in the image, although the Maltese cross are not very perfect. However, after annealing for 10 min, no separate Maltese crosses but lots of imperfect ones are observed in Fig. 1(B) due to the impingement and overlap between each other. During this annealing process, only several crystallites could be formed into perfect spherulites in short time at of the beginning crystallization stage, and then the nucleus of PMT grow fast and impinge to each other forming imperfect spherulites in the end.

Fig. 2 gives the WAXD pattern of crystalline PMT, in which several strong crystalline reflections are observed and the values of 2θ and d_{hkl} are listed in Table 1. Deduced from the structure of the molecular chain of PMT, the chain conformation is ~PZ (plane-zigzag), and the crystal cell dimensions are also calculated and listed in Table 1. It is believed that the PMT crystal cell belongs to the triclinic crystal system.

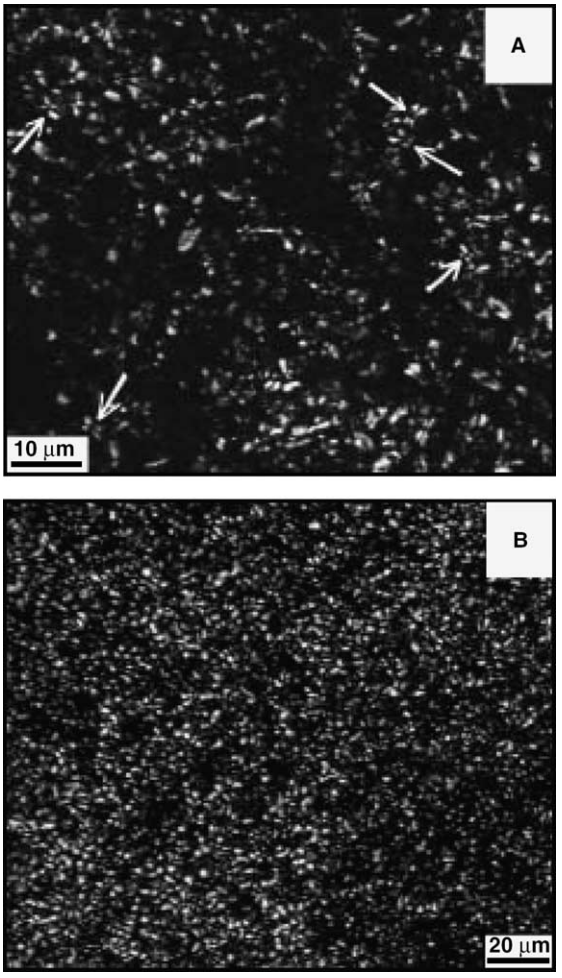

Fig. 1. Polarized optical microscopy of crystalline PMT at different annealing time: (A) 2 min and (B) 10 min.

Table 1
The WAXD parameters and cell dimensions of crystallize PMT

2θ (°)	hkl	d_{hkl} (Å)	a (Å)	b (Å)	c (Å)	α (°)	β (°)	γ (°)
16.74	010	5.29	4.43	5.94	9.42	97.3	126	106.1
24.06	$\bar{1}10$	3.70						
27.90	100	3.20						
32.46	$0\bar{2}1$	2.76						
41.36	$\bar{1}05$	2.18						

3.2. Isothermal crystallization kinetics analysis

3.2.1. Analysis based on the Avrami theory

The relative crystallinity X_t, as a function of crystallization time is defined as

$$X_t = \frac{\int_{t_0}^{t}(\mathrm{d}H/\mathrm{d}T)\mathrm{d}T}{\int_{t_0}^{t_\infty}(\mathrm{d}H/\mathrm{d}T)\mathrm{d}T} = \frac{A_0}{A_\infty}, \quad (1)$$

where $\mathrm{d}H/\mathrm{d}T$ is the rate of heat evolution, t_0 and t_∞ is the time at which crystallization starts and ends, and A_0 and A_∞ are the areas under normalized DSC curves, respectively.

Isothermal crystallization of PMT has been carried out at five different temperatures, 193, 196, 199, 202 and 205 °C, respectively. Fig. 3 shows the exothermal diagrams of isothermal crystallization. It can be seen that as the crystallization temperature (T_c) increases, the exothermal peak of each curve is shifted to longer time, indicating that the T_c is an important influencing factor determining the crystallization time. From the data listed in Table 2, the crystallization enthalpy (ΔH) of PMT increases gradually, implying that the total crystallinity

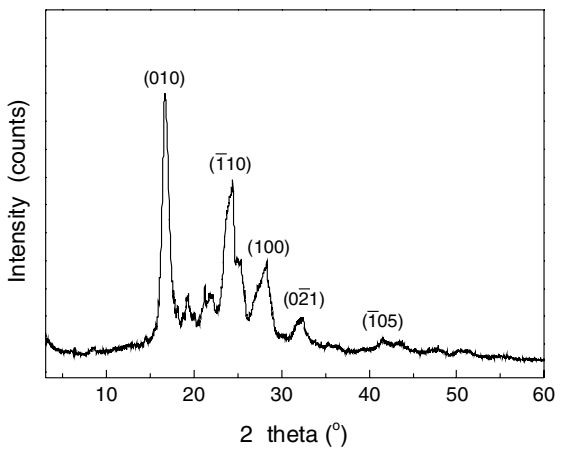

Fig. 2. WAXD patterns of crystalline PMT.

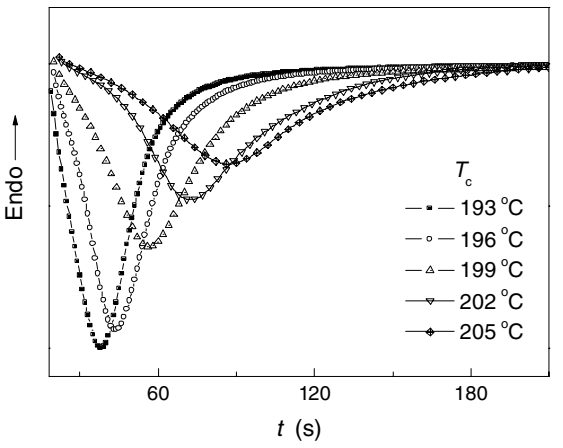

Fig. 3. DSC thermograms of PMT during isothermal crystallization at different designated temperatures.

Table 2
Isothermal crystallization kinetic parameters analyzed by Avrami equation

T_c (°C)	n	K ($\times 10^{-5}$ s^{-n})	t_c (s)	$t_{1/2}$ (s)	ΔH (J/g)
193	2.2	63.1	209	24	46.7
196	2.4	18.6	272	29	50.1
199	2.5	6.5	349	43	52.4
202	2.8	0.9	507	62	54.2
205	2.7	0.7	570	77	55.8

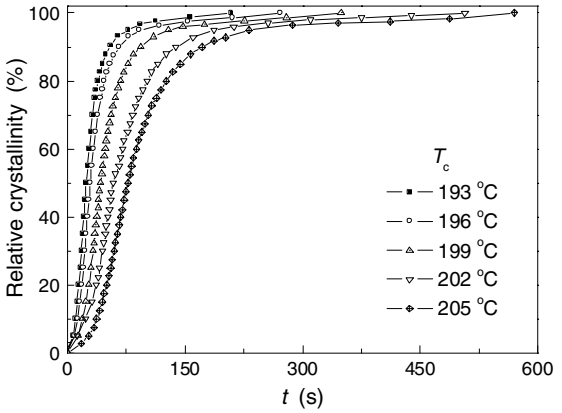

Fig. 4. Development of X_t with t for isothermal crystallization of PMT at different designated temperatures.

increases with increasing T_c. Fig. 4 shows the relative crystallinity (X_t) integrated from Fig. 3 as a function of the crystallization time (t) at various T_c, in which the characteristic sigmoidal isotherms are shifted to right along the time axis with increasing T_c, and the whole crystallization time (t_c) is increasing with the crystallization temperature (Table 2).

In order to compare the crystallization rate at various temperatures, the half-time of crystallization ($t_{1/2}$) versus the T_c is plotted in Fig. 5 and the data is also listed in Table 2. The crystallization rate can be qualitatively compared by the value of $t_{1/2}$. Generally, the smaller the value of $t_{1/2}$, the higher the crystallization rate is. It is observed that the value of $t_{1/2}$ is enhanced with the increase of T_c, indicating that the crystallization rate is decreased by increasing T_c.

Assuming that the relative crystallinity (X_t) increases with the crystallization time (t), the Avrami equation can be used to analyze the isothermal crystallization process of PMT as follows [9,10]:

$$1 - X_t = \exp(-Kt^n), \tag{2}$$

$$\log[-\ln(1 - X_t)] = n \log t + \log K, \tag{3}$$

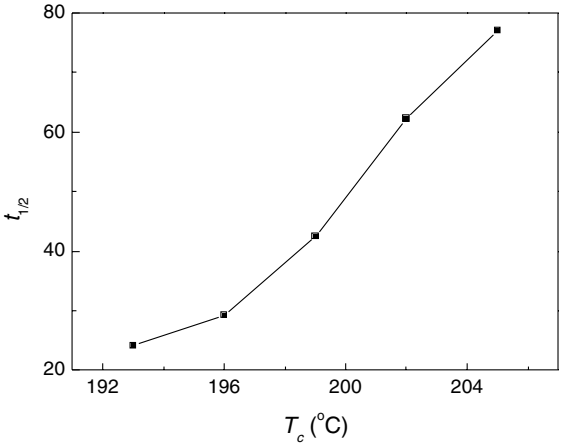

Fig. 5. $t_{1/2}$ versus T_c of isothermal crystallization of PMT.

where X_t is the relative crystallinity at time t; the exponent n is a mechanism constant with a value depending on the type of nucleation and the growth dimension, and the parameter K is a growth rate constant involving both nucleation and the growth rate parameters.

The plots of $\log[-\ln(1 - X_t)]$ versus $\log t$ according to Eq. (3) are shown in Fig. 6, and the Avrami exponent n and the rate constant K can readily be extracted from the Avrami plots. The crystallization process is usually treated as two stages: the primary crystallization stage and the secondary crystallization stage. In Fig. 6, one can see that each curve is composed of two linear sections. This fact indicates the existence of the secondary crystallization. It is generally believed that the secondary crystallization was caused by the crystallization behavior of micro-

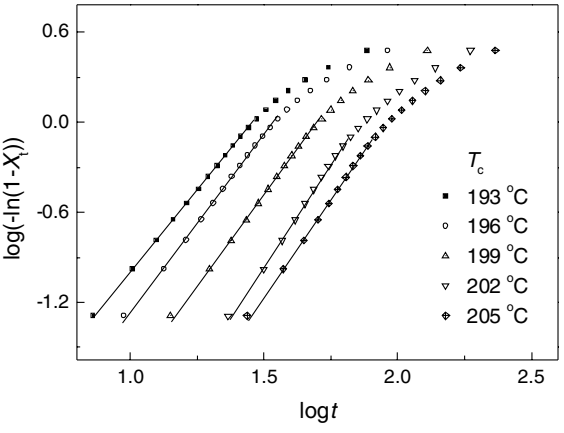

Fig. 6. Plots of $\log[-\ln(1 - X_t)]$ versus $\log t$ for isothermal crystallization of PMT.

crystallites in the range of interface between big spherulites in the later stage of crystallization process [11–13].

In this work, the values of n are between 2 and 3 for PMT, which may be an average value of complex nucleating types and growth dimensions of crystals occurred simultaneous in a crystallization process. According to Avrami theory, for PMT sample, its nucleation type should predominantly be homogenous nucleating and its growth dimensions should predominantly be a two-dimensional growth. As a result, the crystals morphology of PMT should mainly be imperfect spherulites during the isothermal crystallization temperature from 193 to 205 °C.

The crystallization rate parameters (K) of the PMT are listed in Table 2 and compared each other, in which the values of K are gradually decreased with the increasing of T_c. This result suggests that in the isothermal crystallization process, the higher the T_c, the lower the crystallization rate is.

3.2.2. Crystallization activation energy

The crystallization process of the PMT is assumed to be thermally activated. The crystallization rate parameters K can be approximately described by the following Arrhenius equation [14]:

$$K^{1/n} = K_0 \exp(-\Delta E/RT_c), \quad (4)$$

$$(1/n)\log K = \log K_0 - \Delta E/RT_c, \quad (5)$$

where K_0 is the temperature independent pre-exponential factor, R is the gas constant, and ΔE is the crystallization activation energy. ΔE can be determined by the slop coefficient of plots with $(1/n)\log K$ versus $1/T_c$ in Eq. (5) which is shown in Fig. 7. Because it has to release energy when the molten fluid transformed into the crystalline state, the value of ΔE is negative on the basis of the concept of the heat quantity in physical chemistry. In this case, the ΔE value for PMT is found to be −78.8 kJ/mol.

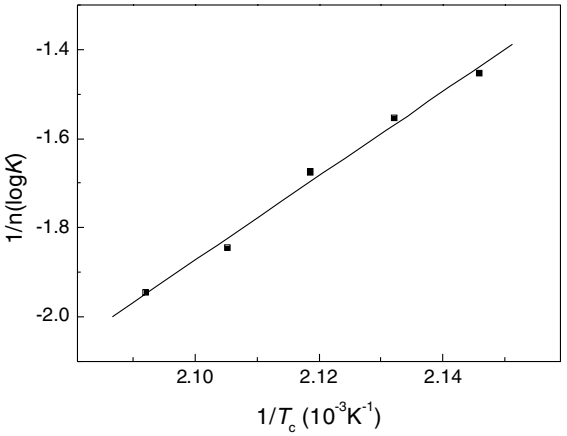

Fig. 7. Plot of $(1/n)\log K_t$ versus $1/T_c$ from the Arrhenius method for isothermal crystallization activation energy of PMT.

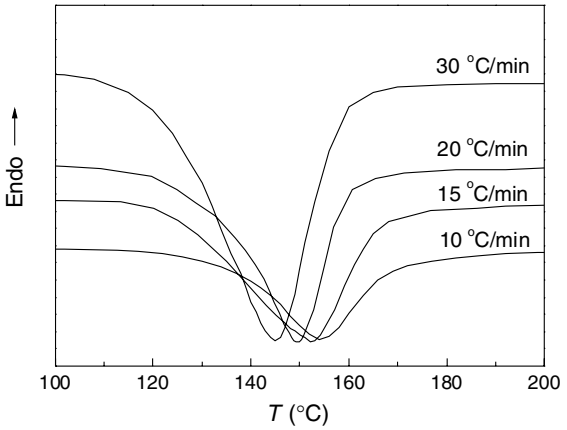

Fig. 8. DSC thermograms of PMT during non-isothermal crystallization at different cooling rates.

Table 3
Non-isothermal crystallization kinetic parameters analyzed by modified Avrami equation

D (°C/min)	T_p (°C)	n	K_t (10^{-8} s^{-n})	K_c (s^{-n})	$t_{1/2}$ (s)	ΔH (J/g)
10	154.5	3.4	0.1	0.13	238.1	35.089
15	151.3	3.3	4.2	0.32	148.8	30.102
20	149.7	3.6	13.4	0.45	75.3	29.476
30	144.7	3.5	61.7	0.62	55.8	19.275

3.3. Non-isothermal crystallization kinetics analysis

3.3.1. Analysis based on the Avrami theory by Jeziorny modified

The non-isothermal crystallization exothermic peaks of PMT at various cooling rates, D, are shown in Fig. 8. The parameters of non-isothermal crystallization are summarized in Table 3. The peak temperature, T_p, shifts to lower temperature region with increasing cooling rates. From the DSC digital information, the relative crystallinity (X_t) is calculated at different temperatures T, and the plots of X_t versus T are shown in Fig. 9. The relationship between temperature T and time t is given by Eq. (6) during the non-isothermal crystallization process, as follows:

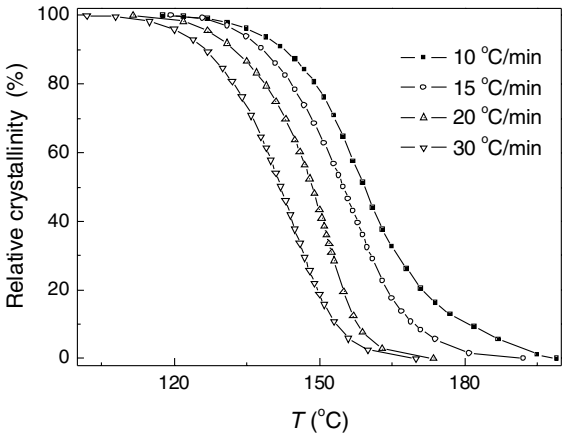

Fig. 9. Relative crystallinity versus temperature for non-isothermal crystallization at different cooling rates.

$$t = \frac{|T_0 - T|}{D}, \tag{6}$$

where t is the crystallization time, T_0 is the temperature at which crystallization begins ($t = 0$), T is the temperature at a crystallization time, and D is the cooling rate. According to Eq. (6), the horizontal T-axis in Fig. 9 can be transformed into the crystallization time t-axis as shown in Fig. 10. It can be seen from Fig. 10 that all these curves have similar sigmoidal shape, and the curvature of the upper parts of the plot is observed to be level off due to the spherulites impingement which already begin from the inflection point of the curves. The characteristic sigmoidal isotherms are shifted to lower temperature or shorter time with increasing cooling rates for completing the crystallization.

Through Fig. 10, we can get the half time of crystallization, $t_{1/2}$, when the X_t are equal to 50%. As listed in Table 3, it can be seen that the $t_{1/2}$ values decrease with the increasing cooling rates, which indicates a progressively faster crystallization rate as the cooling rate increases.

Mandelkern [15] considered that the primary stage of non-isothermal crystallization could be described by the Avrami equation, based on the assumption that the crystallization temperature is constant. Mandelkern obtained the following:

$$1 - X_t = \exp(-K_t t^n), \tag{7}$$

$$\log[-\ln(1 - X_t)] = n \log t + \log K_t, \tag{8}$$

where K_t is a growth rate constant involving both nucleation and growth rate parameters. Jeziorny [16] considered the values of K_t determined by Avrami equation (3) should be adequate as follows:

$$\log K_c = \frac{\log K_t}{D}, \tag{9}$$

where K_c is the kinetic crystallization rate constant.

By using Eqs. (8) and (9), plots of $\log[-\ln(1-X_t)]$ versus $\log t$ of PMT is shown in Fig. 11. Like the process of isothermal crystallization (Fig. 6), nearly each curve shows an initial linear portion and then subsequently turns to a secondary line portion. This fact also indicates the existence of a secondary crystallization, which is caused by spherulite impingement or crowding in the later stage of non-isothermal crystallization process. At the primary stage, the values of the Avrami exponent n and the rate parameters K_t, K_c can be determined

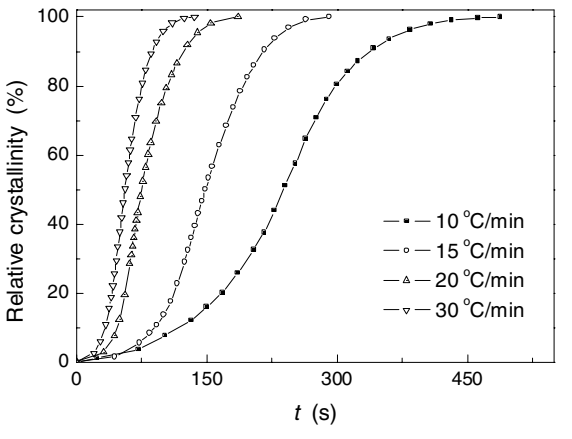

Fig. 10. Relative crystallinity versus time for non-isothermal crystallization at different cooling rates.

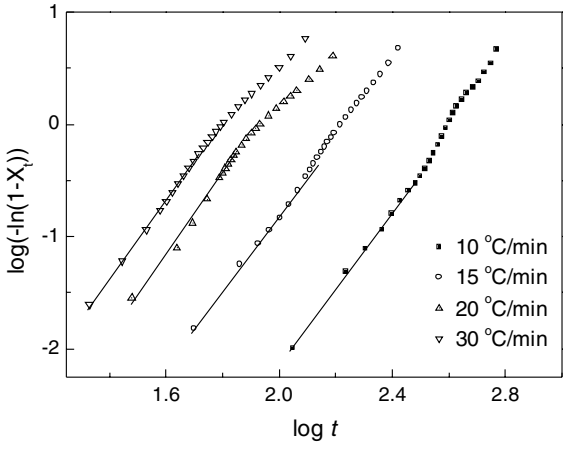

Fig. 11. Plots of $\log[-\ln(1 - X_t)]$ versus $\log t$ for non-isothermal crystallization of PMT.

from the slope and intercept, and these values are listed in Table 3.

At different cooling rates, the Avrami exponents n are about 3.5 ± 0.1, which suggests that the mode at primary stage of the non-isothermal crystallization of spherulite growth is predominantly three-dimensional growth with a homogeneous nucleation mechanism [17]. The value of K_c is increasing with cooling rates, indicating the higher the cooling rate, the higher the crystallization rate is.

3.3.2. Analysis based on the Ozawa theory

Assuming that the non-isothermal crystallization process may be composed of infinitesimally small isothermal crystallization steps, Ozawa [18] shifted the Avrami equation into the process of non-isothermal crystallization, as follows:

$$1 - X_t = \exp\left[-\frac{K(T)}{|D|^m}\right], \tag{10}$$

$$\log[-\ln(1 - X_t)] = \log K(T) - m \log D, \tag{11}$$

where D is the cooling rate, $K(T)$ is a function related to the overall crystallization rate that indicates how fast crystallization proceeds, and m is the Ozawa exponent that depends on the dimension of crystal growth. According to Ozawa's theory, the relative crystallinity at a given temperature can be calculated from these equations. By drawing the plot of $\log[-\ln(1 - X_t)]$ versus $\log D$ at a given temperature, we should obtain a straight line if the Ozawa analysis is valid, and the kinetic parameter m and $K(T)$ can be derived from the slope and the intercept, respectively.

The results of the Ozawa analysis are shown in Fig. 12 and a series of straight lines are obtained,

Table 4
Non-isothermal crystallization kinetic parameters analyzed by Ozawa equation

T (°C)	m	$K(T)$
155	3.0	3.3
150	2.3	2.7
145	1.6	2.1
140	1.2	1.7
135	1.0	1.6

and the values of m and $K(T)$ are listed in Table 4. The values of the m and $K(T)$ are decreased with the decreasing temperature, indicating that the crystal growth is on more dimensions and at fast crystallization rate at higher temperature, whereas it is on lower dimensions and at low crystallization rate at lower temperature. Therefore, an accurate analysis for PMT of the non-isothermal crystallization data could be performed with the Ozawa equation.

3.3.3. Crystallization activation energy

Considering the influence of the various cooling rate D in the non-isothermal crystallization process, Kissinger [19] proposed that the activation energy could be determined by calculating the variation of the crystallization peak with cooling rate:

$$\frac{\mathrm{d}[\ln(D/T_p^2)]}{\mathrm{d}(1/T_p)} = -\frac{\Delta E}{R}, \tag{12}$$

where R is the gas constant and T_p is the crystallization peak temperature. The crystallization activation energy (ΔE) is calculated from the slope of $\ln(D/T_p^2)$ versus $1/T_p$. As shown in Fig. 13, the crystallization activation energy of PMT during non-isothermal crystallization is determined to be

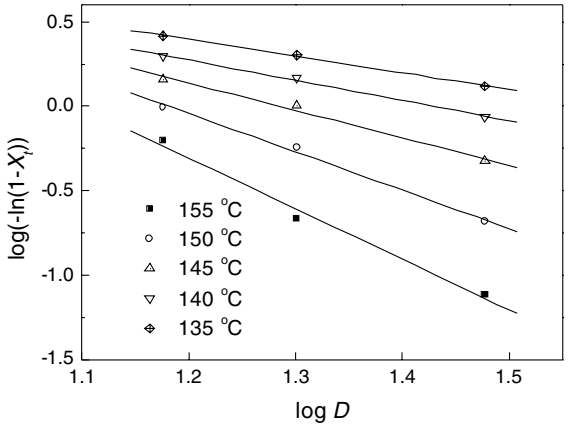

Fig. 12. Ozawa plots of $\log[-\ln(1 - X_t)]$ versus $\log D$ for non-isothermal crystallization of PMT.

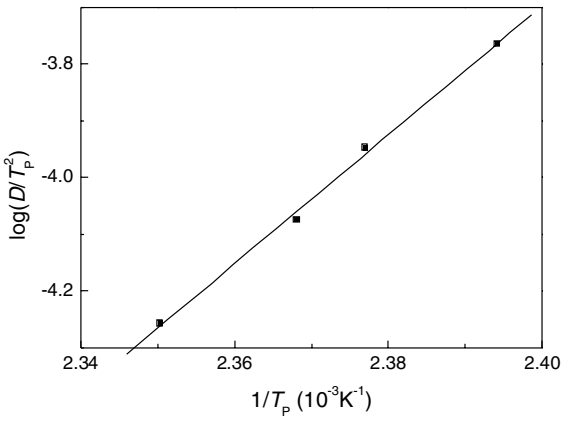

Fig. 13. Plot of $\ln(D/T_p^2)$ versus $1/T_p$ from the Kissinger method for non-isothermal crystallization activation energy of PMT.

−94.5 kJ/mol. Compared with ΔE (−78.8 kJ/mol) in the isothermal crystallization process, the values of ΔE are equal approximately, and experimental result indicates that the research method is correct in the isothermal and non-isothermal crystallization process for PMT.

4. Conclusion

The crystal morphology of PMT is imperfect spherulites with the size of 3–6 μm after annealing from the melt at 200 °C for 10 min, and its crystal cell belongs to the triclinic crystal systems calculated from the WAXD pattern that gives strong crystal reflections.

From the results of the Avrami analysis of isothermal crystallization of PMT, it is believed that the crystallization process is composed of the primary stage and the second stage. At the primary stage, the Avrami exponent n is in the range of 2–3 and the crystal nucleation type and growth dimension should predominantly be homogenous nucleating and two-dimension growth, respectively. The crystallization rate is varied with the temperature of isothermal crystallization, that is, the higher the temperature, the lower the crystallization rate is. The crystallization enthalpy (ΔH) of PMT increases gradually, implying that the total crystallinity increases with increasing T_c.

At the primary stage of the non-isothermal crystallization process, the Avrami exponent, n, is in the range of 3–4, indicates that the crystallization process is predominantly of two- and three-dimensional growth with homogenous nucleation, and it is more complicated than those of isothermal crystallization. The crystallization rate is increased with the cooling rates varied from 10 to 30 °C. The Ozawa theory is also successfully describing the non-isothermal crystallization process, and the Ozawa exponent m is in the range of 1–3 at temperatures from 135 to 155 °C in this case.

Acknowledgements

The authors are grateful to Dr. Gang Wu for supplying the samples and financial support of the Science Foundation of Hebei University.

References

[1] East GC, Morshed M. Polymer 1982;23:1555.
[2] Cimecioglu AL, East GC, Morshed M. J Polym Sci, Part A: Polym Chem 1988;26:2129.
[3] Chuah HH. Chem Fibers Int 1996;46:424.
[4] Gilbert M, Hybart FJ. Polymer 1974;15:407.
[5] Pyda M, Boller A, Grebowicz J, Chuah HH, Lebedev BV, Wunderlich B. J Polym Sci, Part B: Polym Phys 1998;36: 2499.
[6] Huang JM, Chang FC. J Polym Sci Part B: Polym Phys 2000;38:934.
[7] Di Lorenzo ML, Silvestre C. Prog Polym Sci 1999;24:917.
[8] Dangseeyun N, Srimoaon P, Supaphol P, Nithitanakul M. Thermochim Acta 2004;409:63.
[9] Avarami M. J Chem Phys 1940;8:212.
[10] Avarami M. J Chem Phys 1939;7:1103.
[11] Wunderlich B. Macromolecular physics, vol. 2. New York: Academic Press; 1977.
[12] Long Y, Shanks RA, Stachurski ZH. Prog Polym Sci 1995;20:651.
[13] Liu S, Yu Y, Cui Y, Zhang H, Mo Z. J Appl Polym Sci 1998;70:2371.
[14] Cebe P, Hong SD. Polymer 1986;27:1183.
[15] Fava RA. Methods of experimental physics. Polymers, Part B: crystal structure and morphology, vol. 16B. New York: Academic Press, Inc; 1980.
[16] Jeziorny A. Polymer 1978;19:1142.
[17] Bicerano J. J Macromol Sci Rev Macromol Phys 1998; C38:391.
[18] Ozawa T. Polymer 1971;12:150.
[19] Kissinger HE. J Res Natl Stand (US) 1956;57:217.